COURSE 10

QUANTUM FLUCTUATIONS IN ELECTRICAL CIRCUITS

Michel H. Devoret

Service de Physique de l'Etat Condensé
CEA-Saclay, F91191 Gif-sur-Yvette, France

S. Reynaud, E. Giacobino and J. Zinn-Justin, eds.
Les Houches, Session LXIII, 1995
Fluctuations Quantiques
Quantum Fluctuations

Contents

1. Introduction

One usually associates quantum mechanics with microscopic particles such as electrons, atoms or photons and classical mechanics with macroscopic objects such as billiard balls, solar systems and sound waves. In recent years however, the notion has emerged that some systems, referred to as macroscopic quantum systems, have a status intermediate between microscopic particles and classical macroscopic objects [1]. Like billiard balls, they are macroscopic in the sense that they contain a large number of microscopic particles and are "artificial", i.e. built according to certain specifications. However, these macroscopic quantum systems have collective degrees of freedom, analogous to the position of the center-of-mass of the ball, that behave quantum-mechanically. The parameters influencing this quantum behavior are not fundamental, "God-given" constants like the Rydberg energy or the fine structure constant. They are phenomenological parameters which can be tailored by the design of the system. Macroscopic quantum mechanics is a new area of research where novel quantum phenomena that have no equivalent in the microscopic world can be imagined and observed [2].

To make the discussion more concrete, let us imagine a LC oscillator circuit (see Fig. 1a) fabricated with the technology of microelectronic chips. Typical values that can be easily obtained for the inductance and the capacitance are $L = 10$ nH and $C = 1$ pF. They lead to a resonant frequency $\omega_0/2\pi = 1/2\pi\sqrt{LC} \simeq 1.6$ GHz in the microwave range. Nevertheless, because the overall dimensions of the circuit do not exceed a few hundred μm, which is much smaller than the wavelength corresponding to ω_0, the circuit is well in the lumped element limit. It is described with only one collective degree of freedom which is the flux Φ in the inductor. This variable is the electric analog of the position of the mass in a mass-spring mechanical oscillator, the momentum of the mass corresponding to the charge Q on the capacitor. The variables Q and Φ are conjugate coordinates in the sense of Hamiltonian mechanics.

The chip on which this circuit has been patterned is enclosed in a well-shielded copper box anchored thermally to the cold stage of a dilution refrigerator at $T = 20$ mk. With these precautions, the thermal fluctuation energy is smaller than the energy quantum associated with the resonant frequency: $k_B T \ll \hbar\omega_0$. But this latter condition is not sufficient to ensure that Φ needs to be treated as a quantum variable: the width of the energy levels must also be smaller than their separation.

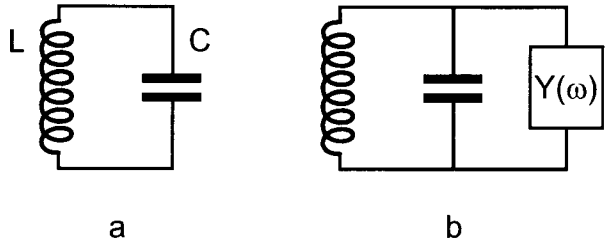

Fig. 1. (a) LC oscillator. (b) LC oscillator connected to an electromagnetic environment represented by an admittance $Y(\omega)$ in parallel with the circuit.

This means that the quality factor of the LC oscillator needs to satisfy $\mathcal{Q} \gg 1$, a constraint on the damping of the oscillator.

Of course, a superconducting metal can be used for the wire of the inductor. But we also need to make measurements on the circuit via leads which can transfer energy in and out the oscillator. The leads and the measuring circuit constitute the electromagnetic environment of the LC oscillator. The strong coupling between the oscillator and its environment is the main limiting factor for the quanticity of Φ. The influence of the environment on the oscillator can be modelled as a frequency dependent admittance $Y(\omega)$ in parallel with the capacitance and the inductance (see Fig. 1b). The environment shifts the oscillator frequency by the complex quantity $\Delta + \frac{i}{2}\omega_0/\mathcal{Q} \simeq \frac{i}{2}\omega_0 Y(\omega_0) Z_0$, where $Z_0 = \sqrt{\frac{L}{C}}$ is the impedance of the elements of the oscillator on resonance. In our example Z_0 has the value 10Ω. We can engineer leads that do not bring too much external noise and at the same time do not load the oscillator too much: a typical value for $|Y(\omega)|^{-1}$ is 100Ω [3], yielding $\mathcal{Q} \simeq 10$.

This example shows how electrical circuits, which are intrinsically fast and flexible, constitute a class of macroscopic quantum systems well adapted to experimental investigations.

However, the particular LC circuit we have considered only displays rather trivial quantum effects. Because it belongs to the class of harmonic oscillators, it is always in the correspondence limit. The average value of the position or the momentum follows the classical equations of motion. Quantum mechanics is revealed in higher moments like the variance of these basic variables, but these higher moments are considerably much more difficult to measure than average quantities since we are dealing with a single quantum system.

Non-trivial and directly observable macroscopic quantum effects appear in circuits which contain at least one non-linear component. A very basic non-linear component is a Josephson tunnel junction. In contrast with most other non-linear electronic devices, its relevant properties remain temperature independent as

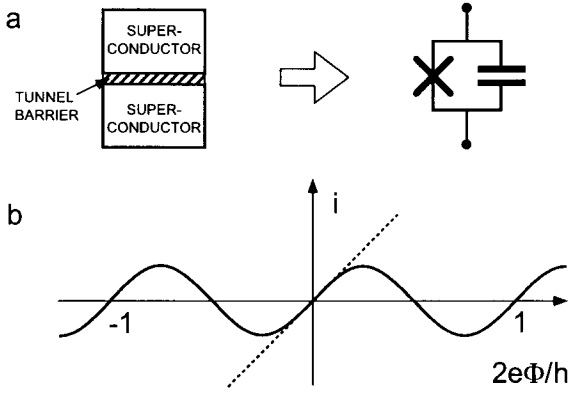

Fig. 2. (a) A Josephson tunnel junction can be modelled as a Josephson tunnel element (cross) in parallel with a capacitor. (b) Current-flux relation of the Josephson element. The dashed line is the current-flux relation of a linear inductance whose value is equal to the effective inductance of the junction.

the temperature is lowered to reach the conditions required for the observation of quantum effects. The Josephson tunnel junction consists of two superconductors separated by a thin oxide layer (see Fig. 2a). It is modelled as a pure superconducting tunnel element (also called Josephson element), which can be thought of as a non-linear inductor (Fig. 2b), in parallel with a capacitance. The latter corresponds to the parallel plate capacitor formed by the two superconductors. The Josephson element is traditionally represented by a cross in circuit diagrams. The origin of the non-linearity of the Josephson element is very fundamental: as we will see, it is associated with the discreteness of charge that tunnels across the thin insulating barrier.

At a temperature of a few tens of mK, all the electrons in the superconducting electrodes on each side of the junction are condensed into Cooper pairs. All internal degrees of freedom in the electrodes are thus frozen and the junction is characterized only by two *a priori* independent collective degrees of freedom: the charge $Q(t)$ on the capacitance and the number $N(t)$ of Cooper pairs having tunneled across the Josephson element. The charge $Q_J(t) = -2eN(t)$ having flown through the Josephson element up to a time t differs from $Q(t)$ if the junction is connected to an electrical circuit. Note that while Q is a continuous variable corresponding to a bodily displacement of the electron fluid in the electrodes with respect to the ion lattice, N is an integer variable. The Josephson element can also be characterized by a flux Φ_J, a position-like variable which generalizes the flux in an inductor and which can be defined as the time integral of the instantaneous

voltage v across the element.

$$\Phi_J(t) = \int_{-\infty}^{t} v(t')\,dt'. \tag{1.1}$$

At time $t = -\infty$, all electromagnetic fields in the circuit are supposed to have been zero and the voltage v includes in particular electromotive forces due to the appearance of magnetic field through the loops of the circuit containing the Josephson junction.

Whereas for an inductance L there is a linear relation between the current $i(t)$ that flows through it and the flux $\Phi(t)$ in it

$$i(t) = \frac{1}{L}\Phi(t) \tag{1.2}$$

the Josephson element is characterized by the following current-flux relation:

$$i(t) = I_0 \sin\left[\frac{2e}{\hbar}\Phi_J(t)\right]. \tag{1.3}$$

As previously mentioned, the scale of non-linearity in this relation is set by the superconducting flux quantum $\hbar/2e$ based on the Cooper pair charge $2e$. The dimensionless combination $\delta = (\hbar/2e)\,\Phi_J$ is known under the esoteric name "gauge invariant phase difference" or simply "phase difference". The presence of $\hbar$ in the argument of the sine function in the current-flux relationship should not obscure the fact that Φ_J is a macroscopic collective variable. For $\Phi_J \ll \hbar/2e$ the tunnel element behaves as an inductor with an effective inductance $L_J = \hbar/(2eI_0)$.

Josephson's unexpected discovery [4] was that the parameter I_0 (and correspondingly L_J) which characterizes the tunnel element is a macroscopic parameter proportional to the area of the junction and the transparency of the tunnel barrier. Typical values for I_0 in experiments on macroscopic quantum effects are in the μA – nA range. Correspondingly, the junction capacitances are in the pF – fF range. These orders of magnitude make characteristic frequencies of the junction in the GHz range. There is a thus a similarity between experiments on quantum effects in Josephson junction systems and cavity QED experiments [5]. Josephson junctions play the role of Rydberg atoms while the rest of the circuit plays the role of the cavity and the preparation/detection apparatuses.

In contrast with the LC oscillator, whose quantum fluctuations are completely decoupled from the average current and voltage that may be present in the oscillator due to an external dc source, the quantum fluctuations of a Josephson junction (or of more complex complex systems involving several junctions) manifest themselves directly in transport experiments during which average voltages or currents are measured in the circuit as a function of external bias sources [6,7]. This relative experimental simplicity has a counterpart, however. Josephson junctions are

so well coupled to their electromagnetic environment that dissipation cannot be treated as a perturbation. In fact, dissipation combines with the non-linearity of tunnel elements to produce qualitatively new quantum effects which are not encountered for example in the almost dissipation-free quantum systems studied in atomic physics. The most spectacular new quantum feature is the localization of position-like degrees of freedom when dissipation exceeds a certain threshold set by the quantum of resistance $h/(2e)^2 \simeq 6.4\ \mathrm{k}\Omega$ [8–10].

This course is not intended as a review of the now important literature on quantum effects in tunnel junction circuits (for a recent snapshot, see for example [10] and [11]). It rather aims at discussing some basic concepts which, in the author's opinion, are important to understand the various points of view adopted in the specialized articles.

Thus, the references given in this course constitute an incomplete and subjective picture of the field. They must be thought of only as entry points in the literature.

This course is organized as follows. In the next section, we explain how the Hamiltonian formalism, which provides a well-treaded path to go from the classical to the quantum description of a system, can be applied to electrical circuits. Whereas the Hamiltonian framework can be straightforwardly applied to the LC oscillator of Fig. 1, it is much less obvious to do so in complicated circuits, in particular with non-linear elements, and we describe a systematic procedure. A thorough understanding of the classical properties of tunnel junction circuits is needed to separate clearly effects due to the non-linear constitutive relation of tunnel elements (which originates from microscopic quantum effects in the junction and can be taken as purely phenomenological) and genuine macroscopic quantum effects originating from quantum fluctuations of macroscopic electrical quantities. We then treat in the following section the quantum mechanics of linear dissipative circuits. We discuss in particular the case of the LC circuit with damping. The quantum fluctuations of this system can be computed analytically and they provide a useful benchmark for the quantum fluctuations in circuits involving Josephson junctions which are treated in the last section.

2. Hamiltonian description of the classical dynamics of electrical circuits

2.1. Non-dissipative circuits

2.1.1. Branch variables

An electrical circuit can be formally described as a network whose branches consist of two-terminal electrical elements such as capacitors, inductors or more complex elements (see example on Fig. 3). We will first restrict ourselves to non-dis-

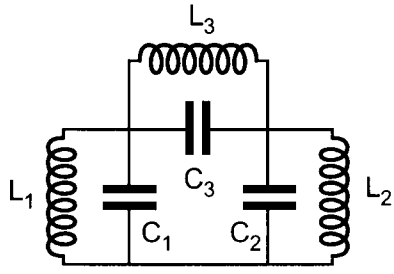

Fig. 3. Example of non-dissipative circuit whose branches consist of linear inductances and capacitances. The nature and number of degrees of freedom of the circuit would not change if the linear elements were replaced by non-linear ones.

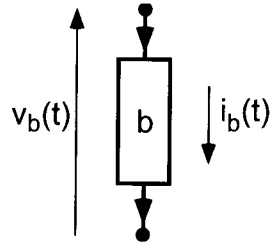

Fig. 4. Sign convention for the voltage and current associated with an arbitrary branch b of an electrical circuit.

sipative elements. However, we allow non-linear elements such as Josephson junctions.

The element of each branch b at time t is characterized by two variables: the voltage $v_b(t)$ across it and the current $i_b(t)$ flowing through it (the branch b has an orientation which determines the sign of voltage and current as shown on Fig. 4). These variables play the role of velocities and forces in mechanical systems, respectively. They can be defined from the underlying electromagnetic fields by the line integrals

$$v_b = \int_{\text{beginning of } b}^{\text{end of } b} \vec{E} \cdot \vec{ds}, \tag{2.1}$$

$$i_b = \frac{1}{\mu_0} \oint_{\text{around } b} \vec{B} \cdot \vec{ds}. \tag{2.2}$$

Because we consider circuits in the lumped element approximation, these definitions make voltages and currents independent of the precise path of integration along which fields are integrated, provided "natural" paths are chosen. These

paths are outside the wire of inductors for the line integral of electric field and outside the dielectric of capacitors for the loop integral of magnetic field. Note that these definitions are sufficiently general to include the contribution to voltages of emf's due to time-varying magnetic fields and the contribution to currents of displacement currents due to time-varying electric fields. Note also that the factor μ_0 in the definition of current comes from our choice of working with SI units throughout this course.

An Hamiltonian description of electrical circuits requires the introduction of branch fluxes and branch charges which are defined from branch voltages and branch currents by

$$\Phi_b(t) = \int_{-\infty}^{t} v_b(t')dt', \tag{2.3}$$

$$Q_b(t) = \int_{-\infty}^{t} i_b(t')dt'. \tag{2.4}$$

The circuit is supposed to have been at rest at time $t = -\infty$ with no voltages and currents. Static bias fields imposed externally on the circuit such as magnetic fields through the inductors are supposed to have been switched on adiabatically from $t = -\infty$ to $t = 0$.

Each element is characterized by a constitutive relation linking current and voltage variations. We must distinguish between capacitive elements for which the relation is of the form

$$v_b = f(Q_b) \tag{2.5}$$

and inductive elements for which the relation is of the form*

$$i_b = g(\Phi_b). \tag{2.6}$$

Usual linear capacitances and inductances are special cases corresponding to $f(Q_b) = Q_b/C$ and $g(\Phi_b) = \Phi_b/L$. As we have seen with Eq. (1.3), a Josephson tunnel junction is an inductive element where g is a sine function.

Since the power flowing into the element of branch b is given by $v_b i_b = v_b \dot{Q}_b = i_b \dot{\Phi}_b$, the energy of capacitive elements is

$$h(Q_b) = \int_0^{Q_b} f(Q)\, dQ \tag{2.7}$$

while the energy of inductive elements is

$$h(\Phi_b) = \int_0^{\Phi_b} g(\Phi)\, d\Phi. \tag{2.8}$$

* We neglect here mutual inductances. In general the current in a given inductive branch is a function of the fluxes in all the inductive branches. Avoiding this complication does not fundamentally alter the formalism.

2.1.2. The degrees of freedom of a circuit

The branch fluxes and charges do not directly constitute the degrees of freedom of the circuit because they are not independent variables. They must follow constraints imposed by the topology of the circuit. These constraints are expressed by Kirchhoff's laws which state that the sum of voltages around a loop l and the sum of currents arriving at a node n should be zero as long as the flux Φ_l through the loop and the charge $\tilde{Q}_n$ of the node remain constant.

$$\sum_{\text{all } b \text{ around } l} \Phi_b = \tilde{\Phi}_l, \tag{2.9}$$

$$\sum_{\text{all } b \text{ arriving at } n} Q_b = \tilde{Q}_n. \tag{2.10}$$

In standard circuit theory, the constraints imposed by Kirchhoff's laws are dealt with by introducing node voltages or loop currents, either of which can constitute a set of independent degrees of freedom. In the following, we will rather emphasize the node variable representation which is often more adapted to the treatment of circuits involving tunnel elements like Josephson junctions.

Unlike branch variables, *node variables are electrical quantities which depend on a particular description of the topology of the circuit.* The description of the topology of the circuit is given as follows. One node is first chosen as a reference node called "ground". The remaining nodes of the network are referred as "active nodes". From the ground node one then constructs a "spanning tree" by choosing a set of branches such that every active node of the network is connected to the ground node by only one path along the tree (see example of spanning tree on Fig. 5). The remaining branches are "closure branches". Each of them defines a loop obtained by joining the two ends of the branch by the minimal path on the spanning tree. These "irreducible loops" form a basis set from which each loop of the network can be constructed. The spanning tree thus partitions the branches of the network into two sets: the set T of branches belonging to the spanning tree, each of which is associated with an active node, and the set C of closure branches, each of which is associated with an irreducible loop.

The choice of ground node and spanning tree is analogous to the choice of a particular gauge in electromagnetic field theory and to the choice of a system of position coordinates in classical mechanics.

We can now introduce the flux ϕ_n of a node n which is defined by the time integral of the voltage measured along the path connecting the node to the ground on the spanning tree. One has

$$\phi_n = \sum_b S_{nb} \Phi_b. \tag{2.11}$$

In this last definition, the matrix element S_{nb} is 1, -1 or 0 depending on

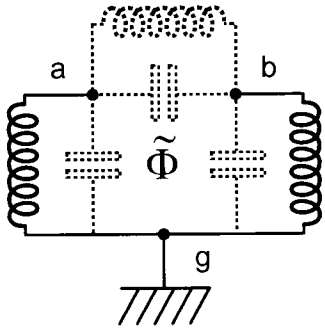

Fig. 5. Example of spanning tree for the circuit of Fig. 3. Closure branches are in dashed line. The constant $\tilde{\Phi}$ is the magnetic flux through the loop formed by the three inductors.

whether the path joining the ground to n follows b with the proper orientation, the opposite orientation or does not follow b. Conversely, the flux of a branch b can be obtained from the fluxes of the end nodes n and n' of the branch, provided that the static fluxes through the loops corresponding to the closure branches are given.

$$\Phi_{b\in\mathsf{T}} = \phi_n - \phi_{n'}, \tag{2.12}$$

$$\Phi_{b\in\mathsf{C}} = \phi_n - \phi_{n'} + \tilde{\Phi}_{l(b)}. \tag{2.13}$$

Instead of node fluxes, one could have introduced irreducible loop charges obtained by taking the time integral of the current in the closure branches. We would then arrive at the loop variable representation which is the dual of the node variable representation.

It is important to realize that the concept of node flux is closely related to the condensate phase φ at a given point of a superconducting circuit. The two quantities satisfy the relation

$$\varphi = \frac{2e}{\hbar}\phi \bmod 2\pi.$$

The node flux ϕ can be defined for any circuit, whether it is superconducting or not, whereas the phase φ is usually introduced only in superconducting systems.

2.1.3. Lagrangian of a circuit

We can now obtain the equations of motion of the circuit by equating, for each active node, two currents: i) the sum of currents arriving from the inductive elements connected to that node and ii) the sum of currents going into the capacitive

elements connected to that node. As an example, the circuit of Fig. 3, for which one can choose as the two active nodes the nodes a and b, has the following equations of motion:

$$C_1\ddot{\phi}_a + C_3\left(\ddot{\phi}_a - \ddot{\phi}_b\right) = \frac{\phi_a}{L_1} + \frac{\phi_a - \phi_b + \tilde{\Phi}}{L_3}, \tag{2.14}$$

$$C_2\ddot{\phi}_b + C_3\left(\ddot{\phi}_b - \ddot{\phi}_a\right) = \frac{\phi_b}{L_2} + \frac{\phi_b - \phi_a - \tilde{\Phi}}{L_3}. \tag{2.15}$$

It is easy to show that these equations of motions are the Euler–Lagrange equations associated with a Lagrangian obtained by subtracting the energy of the inductive elements from the energy of the capacitive elements, these energies being expressed as functions of the node variables ϕ_n and their time derivative $\dot{\phi}_n$. For the circuit of Fig. 3 and the choice of spanning tree of Fig. 5 the Lagrangian is

$$\mathcal{L}\left(\phi_a, \dot{\phi}_a, \phi_b, \dot{\phi}_b\right) = \frac{C_1\dot{\phi}_a^2}{2} + \frac{C_2\dot{\phi}_b^2}{2} + \frac{C_3\left(\dot{\phi}_a - \dot{\phi}_b\right)^2}{2} - \left[\frac{\phi_a^2}{2L_1} + \frac{\phi_b^2}{2L_2} + \frac{\left(\phi_a - \phi_b + \tilde{\Phi}\right)^2}{2L_3}\right]. \tag{2.16}$$

Our approach for the construction of the Lagrangian of a circuit generalizes the work of Yurke and Denker [12].

2.1.4. Node charges: the conjugate momenta of node fluxes

From the Lagrangian we can now define conjugate momenta of node fluxes by the usual relation

$$q_n = \frac{\partial \mathcal{L}}{\partial \dot{\phi}_n}. \tag{2.17}$$

The node charge q_n is the algebraic sum of the charges on the capacitances connected to node n (in the loop variable representation the conjugate momenta of the loop charge is the sum of the fluxes in the inductors of the loop). Since for all circuits of interest each active node is connected to a capacitance (in a real circuit there is always some parasitic capacitance between nodes), the q_n are always defined [13] and we can perform a Legendre transformation of the Lagrangian with respect to q_n. We obtain by this systematic procedure an Hamiltonian of the circuit.

2.1.5. Hamiltonian of a circuit

Taking again the example of the circuit of Fig. 3, we can apply this procedure and obtain the following Hamiltonian

$$\mathcal{H}(\phi_a, q_a, \phi_b, q_b) = \frac{1}{C_1C_2 + C_1C_3 + C_2C_3}\left[\frac{(C_2 + C_3)\,q_a^2}{2} + \frac{(C_1 + C_3)\,q_b^2}{2} + \frac{C_3\,(q_a - q_b)^2}{2}\right] + \left[\frac{\phi_a^2}{2L_1} + \frac{\phi_b^2}{2L_2} + \frac{(\phi_a - \phi_b + \tilde{\Phi})^2}{2L_3}\right]. \tag{2.18}$$

The first term in $\mathcal{H}$ is the electrostatic energy of the circuit expressed as a function of the node charges while the second term is the magnetic energy expressed as a function of node fluxes. This structure is a general characteristic of the Hamiltonian of a circuit in the node variable representation and does not depend on whether the elements are linear or not. The Hamiltonian formulation shows clearly the role of $\tilde{\Phi}$ as an offset term in the magnetic energy. In the case of a linear inductor, the effect of this term is simply to induce an offset dc current. However, in the case of non-linear inductors like Josephson junctions, this term changes the dynamics of the circuit.

One can easily verify that Hamilton's equations

$$\dot{\phi}_n = \frac{\partial \mathcal{H}}{\partial q_n} \tag{2.19}$$

$$\dot{q}_n = -\frac{\partial \mathcal{H}}{\partial \phi_n} \tag{2.20}$$

are equivalent to the equations of motion (2.14) and (2.15) .

It is important to note that although the Hamiltonian of the circuit always gives its total energy, its functional form depends on the particular choice of spanning tree, even when the choice of a representation in terms of node variables or loop variables has been made.

However, the Poisson bracket [14] of the flux and charge of a branch is independent of the choice of the spanning tree and is always unity.

$$\{\Phi_b, Q_b\} = \sum_n \frac{\partial \Phi_b}{\partial \phi_n}\frac{\partial Q_b}{\partial q_n} - \frac{\partial Q_b}{\partial \phi_n}\frac{\partial \Phi_b}{\partial q_n} = 1. \tag{2.21}$$

2.1.6. Mechanical analogy

In the node variable representation, the node fluxes play the role of position coordinates and the node charges the role of momentum coordinates. The electrostatic

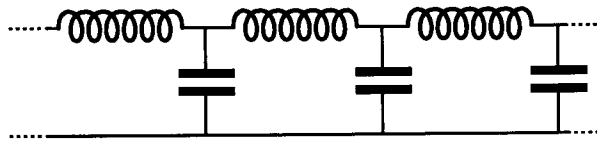

Fig. 6. LC ladder circuit. In the limit of an infinite number of elements, it can model the propagation of the TEM mode of a coaxial transmission line.

energy plays the role of the kinetic energy and the magnetic energy plays the role of the potential energy. However, the form of the Hamiltonian of Eq. (2.18) with electrostatic cross-terms shows that the particular circuit of Fig. 3 has no direct mechanical analog. In the cases where the capacitances are only connected between the active nodes and ground, they can be interpreted as the masses of the active nodes and a direct mechanical analog can be found for the circuit. The inductors then correspond to elastic coupling interactions between the nodes.

2.1.7. Fields to circuits, circuits to fields

Distributed electromagnetic systems can often be caricatured by lumped element circuits which retain the properties of the lowest frequency modes. The link between a microwave cavity and an LC oscillator is very well discussed by Feynman [15]. Thus inductors and capacitors are "bottles" for magnetic and electric fields respectively. On the other hand, if one considers infinite circuits, one can obtain lattice versions of electromagnetism. A simple example is the infinite LC ladder (see Fig. 6) which sustains propagating modes that are equivalent, in the limit of wavelengths long compared with the unit cell, to the TEM modes of a coaxial transmission line. The Hamiltonian formulation is useful in the exploration of such correspondences.

2.2. Circuits with linear dissipative elements

2.2.1. The Caldeira–Leggett model

We would like now to treat circuits with linear dissipative elements like resistors. It would seem that the Hamiltonian formalism is powerless to treat a dissipative system, whose behavior is irreversible, since Hamilton's equations of motion (2.19) and (2.20) are invariant upon time reversal. However this reversibility problem can be solved by slightly extending the formalism. This extension has in fact been made recurrently throughout the history of theoretical physics. We will present here a particularly clear and useful version known as the Caldeira–Leggett model [16] which applies to systems with linear dissipation.

The essence of the Caldeira–Leggett model is to replace, in the context of electrical circuits, a linear dissipative element characterized by a frequency dependent

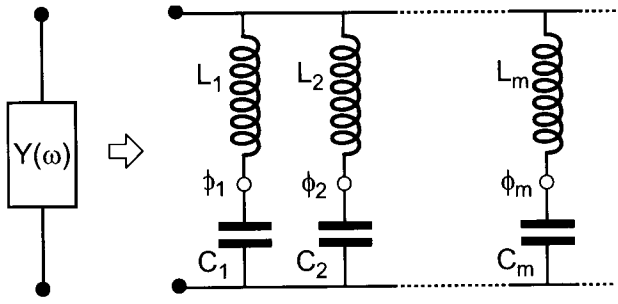

Fig. 7. Caldeira–Leggett model of an admittance $Y(\omega)$.

admittance $Y(\omega)$ by an infinite set of LC oscillators in parallel (see Fig. 7). The internal degrees of freedom of the admittance can be thought of as the fluxes of the intermediate nodes of the LC oscillators (open dots in Fig. 7). It is the passage from a finite number of degrees of freedom to an infinite one that reconciles the irreversible behavior on physical time scales and the formal reversibility of Hamilton's equations of motion.

The reversibility problem appears when one notices that for every oscillator m in the series, the admittance given by the usual combinatorial rules of circuit theory

$$Y_m(\omega) = \left[jL_m\omega + \frac{1}{jC_m\omega} \right]^{-1} \tag{2.22}$$

is purely imaginary while $Y(\omega)$ has both a real and imaginary part (we use here the symbol

$$j = -\sqrt{-1} = -i \tag{2.23}$$

of electricians but with an opposite value to ensure later compatibility with the sign convention of quantum mechanics concerning Fourier transforms). This manifestation of the reversibility problem disappears by extending the notion of admittance function to complex frequencies.

Let us recall that $Y(\omega)$ is defined from the relationship between the voltage across a linear element and the current flowing across it

$$i(t) = \int_{-\infty}^{+\infty} dt' \, \tilde{Y}(t') \, v(t - t'), \tag{2.24}$$

$$Y(\omega) = \int_{-\infty}^{+\infty} dt \, \tilde{Y}(t) \exp(i\omega t). \tag{2.25}$$

We can define an extension of $Y(\omega)$ by

$$Y[\omega + i\eta] = \int_{-\infty}^{+\infty} dt\, \tilde{Y}(t) \exp[i(\omega + i\eta)t] \tag{2.26}$$

(there is no problem at $t \to -\infty$ since $\tilde{Y}(t)$ is a causal function).

All information on the shape of $\tilde{Y}(t)$ after $t \sim \eta^{-1}$ is erased in $Y[\omega + i\eta]$. Let us now define the generalized admittance function by

$$Y[\omega] = \lim_{\substack{\eta \to 0 \\ \eta > 0}} Y[\omega + i\eta]. \tag{2.27}$$

We find that the generalized admittance for the nth oscillator is given by

$$Y_m[\omega] = y_m \left\{ \frac{\pi}{2} \omega_m [\delta(\omega - \omega_m) + \delta(\omega + \omega_m)] + \frac{i}{2} \left[\text{p.p.} \left(\frac{\omega_m}{\omega - \omega_m} \right) + \text{p.p.} \left(\frac{\omega_m}{\omega + \omega_m} \right) \right] \right\}, \tag{2.28}$$

where $\omega_m = 1/\sqrt{L_m C_m}$ and $y_m = \sqrt{C_m/L_m}$. It has both a real and an imaginary part. The idea of Caldeira and Leggett thus consists in replacing the smooth $\text{Re}[Y(\omega)]$ function by an infinitely dense comb of δ functions. Mathematically this corresponds to the following relations between $Y(\omega)$ and the series of oscillators:

$$\omega_{m \neq 0} = m\Delta\omega, \tag{2.29}$$

$$y_{m \neq 0} = \text{Re}[Y(m\Delta\omega)], \tag{2.30}$$

$$L_0 = \frac{1}{\lim_{\omega \to 0} j\omega Y(\omega)}, \tag{2.31}$$

$$L_{m \neq 0} = \frac{1}{y_m \omega_m}, \tag{2.32}$$

$$C_{m \neq 0} = \frac{y_m}{\omega_m}, \tag{2.33}$$

$$Y_m[\omega] = \left[jC_m(\omega + i\eta) + \frac{1}{jL_m(\omega + i\eta)} \right]^{-1}, \tag{2.34}$$

$$Y[\omega + i\eta] = \frac{i}{L_0(\omega + i\eta)} + \lim_{\Delta\omega \to 0} \sum_{m=1}^{\infty} Y_m[\omega + i\eta]; \quad \eta > 0. \tag{2.35}$$

It is important to note that the Caldeira–Leggett model does not constitute a representation of the internal workings of a dissipative element. It is helpful only

to calculate the influence that such an element will have for the rest of the circuit. We calculate this influence by adding to the Hamiltonian of the rest of the circuit the Hamiltonian $\mathcal{H}_Y$ of the admittance

$$\mathcal{H}_Y = \sum_m \left[\frac{q_m^2}{2C_m} + \frac{(\phi_m - \phi)^2}{2L_m} \right]. \tag{2.36}$$

This Hamiltonian has been written in the node representation where the ground has been chosen on one terminal of the admittance. The node flux ϕ corresponds to the other terminal of the admittance while the node fluxes ϕ_m correspond to the intermediate nodes of the LC oscillators. The charges q_m on the capacitances C_m are the momenta conjugate to ϕ_m.

2.2.2. *Voltage and current sources*

Sources of voltages and current can also be treated by the Hamiltonian formalism. A voltage source can be represented as a large capacitor C_S in which is stored initially a large charge Q_S such that $Q_S/C_S = V$ in the limit $C_S \to \infty$. Likewise a current source can be seen represented by large inductor L_S in which is stored initially a large flux Φ_S.

2.2.3. *The classical fluctuation–dissipation theorem*

The value of the Caldeira–Leggett model becomes apparent when we use it to derive the fluctuation–dissipation theorem. Suppose that the admittance $Y(\omega)$, which we suppose in thermal equilibrium at temperature T, is short-circuited. In that case the variable ϕ in the Hamiltonian (2.36) is identically zero and all the oscillators become independent. The current $i(t)$ through the short is zero on average but will fluctuate. We can easily calculate the spectral density of these fluctuations by setting to $\frac{1}{2}k_BT$ the average value of each energy term in the Hamiltonian (2.36). For each oscillator m we can obtain the correlation function of the charge on the capacitance C_m

$$\langle q_m(t) q_m(0) \rangle = C_m k_B T \cos(\omega_m t) . \tag{2.37}$$

The correlation function of the current through the mth oscillator is therefore

$$\langle i_m(t) i_m(0) \rangle = -\frac{d^2}{dt^2} \langle q_m(t) q_m(0) \rangle = y_m \omega_m k_B T \cos(\omega_m t) . \tag{2.38}$$

Using the relation (2.28) we can rewrite this relation as

$$\langle i_m(t) i_m(0) \rangle = \frac{k_B T}{\pi} \int d\omega \, \mathrm{Re}\,(Y_m[\omega]) \exp(-i\omega t) . \tag{2.39}$$

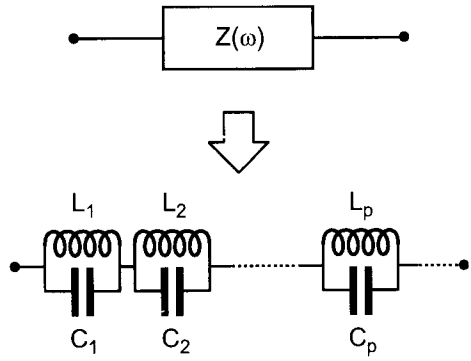

Fig. 8. Caldeira–Leggett representation of an impedance.

Since all the oscillators are independent, we can add their correlation functions to obtain the correlation of the current through the short

$$\langle i(t)i(0)\rangle = \frac{k_B T}{\pi}\int d\omega \,\mathrm{Re}\,(Y[\omega])\exp(-i\omega t)\,. \tag{2.40}$$

We finally obtain the spectral density of current fluctuations in equilibrium defined by

$$S_I(\omega) = \int d\omega \,\langle i(t)i(0)\rangle \exp(i\omega t) \tag{2.41}$$

in terms of the impedance function (Nyquist theorem)

$$S_I = 2k_B T\,\mathrm{Re}\,(Y[\omega])\,. \tag{2.42}$$

The spectral density of thermal equilibrium voltage fluctuations across a linear dissipative element can be obtained as a function of its impedance $Z(\omega) = [Y(\omega)]^{-1}$ in a similar manner. Using the Caldeira–Leggett representation of an impedance (see Fig. 8) and the loop variable representation we obtain

$$S_V = 2k_B T\,\mathrm{Re}\,(Z[\omega])\,. \tag{2.43}$$

We will see in the next section how the quantum treatment of dissipation modifies the results (2.42) and (2.43).

3. Quantum mechanics of linear dissipative circuits

3.1. Quantum description of electrical circuits

The passage from the classical to the quantum description of electrical circuits is straightforward in the framework of the Hamiltonian description developed in the

preceding section. The classical variables are replaced by corresponding operators and the Hamiltonian function is replaced by a function of operators:

$$\begin{aligned} \phi &\to \widehat{\phi}, \\ q &\to \widehat{q}, \\ \mathcal{H} &\to \widehat{\mathcal{H}}. \end{aligned} \tag{3.1}$$

The operators corresponding to the position coordinates all commute and define an Hilbert space. However, commutation relations are imposed on pairs of operators corresponding to conjugate variables. In the node variable representation, the commutator of the node fluxes and conjugate node charges is:

$$\left[\widehat{\phi}_n, \widehat{q}_n\right] = i\hbar. \tag{3.2}$$

This relation just follows from the fact that node fluxes play the role of position coordinates while nodes charges play the role of momentum coordinates. More generally, as shown by Dirac[18], the value of a classical Poisson bracket imposes the value of the corresponding commutator

$$\{A, B\} \to \frac{1}{i\hbar}\left[\widehat{A}, \widehat{B}\right]. \tag{3.3}$$

It follows that the flux and the charge of a branch have the commutator

$$\left[\widehat{\Phi}_b, \widehat{Q}_b\right] = i\hbar \tag{3.4}$$

even if they are not conjugate coordinates.

3.2. Useful relations

Usual relations of quantum mechanics can be adapted to electrical systems. We thus get

$$\frac{\partial \widehat{A}/\partial \widehat{\phi}_n}{\left[\widehat{A}, \widehat{q}_n\right]} = \frac{1}{i\hbar}, \tag{3.5}$$

$$\frac{\partial \widehat{A}/\partial \widehat{q}_n}{\left[\widehat{A}, \widehat{\phi}_n\right]} = \frac{-1}{i\hbar}, \tag{3.6}$$

$$\frac{\partial \widehat{A}/\partial t}{\left[\widehat{A}, \widehat{\mathcal{H}}\right]} = \frac{1}{i\hbar}. \tag{3.7}$$

The sign of the right-hand side in these relations can be obtained by matching the vertical order of the variables on the left-hand side to the order of variables in the columns of the following mnemonic table:

$$\left|\begin{array}{ccc} \widehat{\phi}_n & \longleftrightarrow & t \\ \downarrow & & \downarrow \\ \widehat{q}_n & \longleftrightarrow & \widehat{\mathcal{H}} \end{array}\right| .$$

The integral form of these relations will also be useful:

$$A(t) = \mathrm{e}^{\frac{i\widehat{\mathcal{H}}t}{\hbar}} A(0)\, \mathrm{e}^{-\frac{i\widehat{\mathcal{H}}t}{\hbar}}, \tag{3.8}$$

$$\mathrm{e}^{\frac{i\widehat{\phi}_n q}{\hbar}} \widehat{q}_n \mathrm{e}^{-\frac{i\widehat{\phi}_n q}{\hbar}} = \widehat{q}_n - q, \tag{3.9}$$

$$\mathrm{e}^{\frac{i\widehat{q}_n \phi}{\hbar}} \widehat{\phi}_n \mathrm{e}^{-\frac{i\widehat{q}_n \phi}{\hbar}} = \widehat{\phi}_n + \phi. \tag{3.10}$$

In order to simplify notations, we will, from now on, drop the hat on operators. We will of course make sure that the distinction between operators and c-numbers can be made from the context.

3.3. The quantum LC oscillator

The LC oscillator of Fig. 1 can now be treated quantum mechanically. This circuit with only one active node has a trivial topology. We can immediately adapt well-known textbook results on the harmonic oscillator. Taking as variables the integral ϕ of the voltage across the inductor and the corresponding charge q on the capacitor we have the Hamiltonian

$$\mathcal{H} = \frac{q^2}{2C} + \frac{\phi^2}{2L}. \tag{3.11}$$

Introducing the usual annihilation and creation operators such that

$$\left[c, c^\dagger\right] = 1 \tag{3.12}$$

we have

$$\phi = \sqrt{\frac{\hbar Z_0}{2}} \left(c + c^\dagger\right), \tag{3.13}$$

$$q = \frac{1}{i}\sqrt{\frac{\hbar}{2Z_0}} \left(c - c^\dagger\right), \tag{3.14}$$

$$\mathcal{H} = \frac{\hbar\omega_0}{2}\left(c^\dagger c + c c^\dagger\right) = \hbar\omega_0 \left(c^\dagger c + \tfrac{1}{2}\right), \tag{3.15}$$

where, as in section 1,

$$\omega_0 = \sqrt{\frac{1}{LC}},$$

$$Z_0 = \sqrt{\frac{L}{C}}. \tag{3.16}$$

Using Eq. (3.8) and the relation

$$\langle A \rangle = \mathrm{tr}\left[A \mathrm{e}^{-\beta \mathcal{H}}\right], \tag{3.17}$$

where $\beta = (k_B T)^{-1}$, we can calculate the flux-flux correlation function in thermal equilibrium $\langle \phi(t)\, \phi(0) \rangle$. We arrive at

$$\langle \phi(t)\, \phi(0) \rangle = \frac{\hbar Z_0}{2} \left(\langle c^\dagger c \rangle \mathrm{e}^{+i\omega_0 t} + \langle c c^\dagger \rangle \mathrm{e}^{-i\omega_0 t} \right) \tag{3.18}$$

and from

$$\langle c^\dagger c \rangle = \frac{1}{\mathrm{e}^{\beta\hbar\omega_0} - 1} = \frac{1}{2} \coth\left(\frac{\beta\hbar\omega_0}{2}\right) - \frac{1}{2} = n(\omega_0),$$

$$\langle c c^\dagger \rangle = \frac{1}{1 - \mathrm{e}^{-\beta\hbar\omega_0}} = -n(-\omega_0) = n(\omega_0) + 1. \tag{3.19}$$

we get finally

$$\langle \phi(t)\, \phi(0) \rangle = \frac{\hbar Z_0}{2} \left[\coth\left(\frac{\beta\hbar\omega_0}{2}\right) \cos\omega_0 t - i \sin\omega_0 t \right]. \tag{3.20}$$

Setting $t = 0$ we get the variance of flux fluctuations

$$\langle \phi^2 \rangle = \frac{\hbar Z_0}{2} \coth\left(\frac{\beta\hbar\omega_0}{2}\right), \tag{3.21}$$

which interpolates between the zero-point fluctuations result $\langle \phi^2 \rangle = \hbar Z_0/2$ and the high temperature ($k_B T \gg \hbar\omega_0$) result $\langle \phi^2 \rangle = k_B T C$.

From $\langle q(t)\, q(0) \rangle = -C^2 d^2 \langle \phi(t)\, \phi(0) \rangle / dt^2$ we also get the variance of charge fluctuations

$$\langle q^2 \rangle = \frac{\hbar}{2Z_0} \coth\left(\frac{\beta\hbar\omega_0}{2}\right). \tag{3.22}$$

An important remark can be made: Not only does Eq. (3.20) predict that the amplitude of fluctuations saturates at low temperature (well-known zero-point fluctuations) but it also predicts that the quantum correlation function is not real! The Fourier transform of the correlation function thus cannot be interpreted as a directly measurable spectral density as is the case classically. Let us now discuss the case of a general impedance to further examine this point.

Introducing the generalized impedance function of an LC oscillator

$$Z_{\mathrm{LC}}[\omega] = Z_0 \left\{ \frac{\pi}{2}\omega_0 [\delta(\omega-\omega_0)+\delta(\omega+\omega_0)] + \frac{i}{2}\left[\mathrm{p.p.}\left(\frac{\omega_0}{\omega-\omega_0}\right) + \mathrm{p.p.}\left(\frac{\omega_0}{\omega+\omega_0}\right)\right]\right\} \tag{3.23}$$

we can rewrite (3.20) as

$$\langle \phi(t)\,\phi(0)\rangle = \frac{\hbar}{2\pi}\int \frac{d\omega}{\omega}\left[\coth\left(\frac{\beta\hbar\omega}{2}\right)+1\right]\mathrm{Re}\,(Z_{\mathrm{LC}}[\omega])\exp -i\omega t. \tag{3.24}$$

3.4. The quantum fluctuation dissipation theorem

We can now obtain the quantum correlation function of the branch flux across an arbitrary generalized impedance by using the Caldeira–Leggett representation of Fig. 8. We simply add the contribution of all the oscillators and since the correlation function is a linear function of the real part of the impedance we directly obtain a result of central importance:

$$\langle \Phi(t)\,\Phi(0)\rangle = \frac{\hbar}{2\pi}\int_{-\infty}^{+\infty}\frac{d\omega}{\omega}\left[\coth\left(\frac{\beta\hbar\omega}{2}\right)+1\right]\mathrm{Re}\,(Z[\omega])\exp -i\omega t. \tag{3.25}$$

If we now introduce the spectral density of quantum fluctuations

$$C(\omega) = \int_{-\infty}^{+\infty} dt\,\langle \Phi(t)\,\Phi(0)\rangle \exp i\omega t \tag{3.26}$$

we get the frequency domain relation

$$C(\omega) = \frac{\hbar}{\omega}\left[\coth\left(\frac{\beta\hbar\omega}{2}\right)+1\right]\mathrm{Re}\,(Z[\omega]) \tag{3.27}$$

which is also called the quantum fluctuation dissipation theorem [19]. Note again that in contrast with a classical spectral density of fluctuations $C(-\omega) \neq C(\omega)$.

How should we interpret $C(\omega)$? To make easier the comparison with the classical case let us calculate the voltage-voltage spectral density

$$U(\omega) = \int_{-\infty}^{+\infty} dt\,\langle \dot{\Phi}(t)\,\dot{\Phi}(0)\rangle \exp i\omega t \tag{3.28}$$

which is related to $C(\omega)$ by $U(\omega) = \omega^2 C(\omega)$

$$U(\omega) = \hbar\omega\left[\coth\left(\frac{\beta\hbar\omega}{2}\right)+1\right]\mathrm{Re}\,(Z[\omega]). \tag{3.29}$$

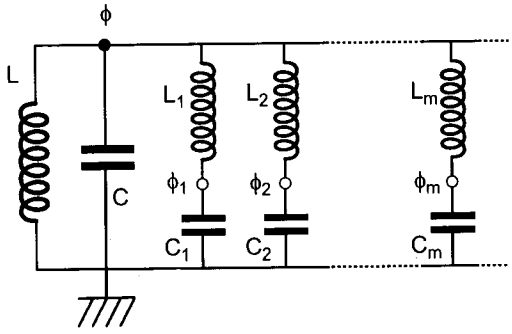

Fig. 9. Caldeira–Leggett representation of the damped LC circuit of Fig. 1b.

In the various limits $U(\omega)$ is given by

$$\begin{aligned} |\hbar\omega| \ll k_B T \quad & U(\omega) = 2k_B T \,\mathrm{Re}\,(Z[\omega])\,, \\ \hbar\omega \gg k_B T \quad & U(\omega) = \hbar\omega \,\mathrm{Re}\,(Z[\omega])\,, \\ \hbar\omega \ll -k_B T \quad & U(\omega) = 0. \end{aligned} \tag{3.30}$$

3.5. Interpretation of the quantum spectral density

The form of U in the quantum limit $|\hbar\omega| \gg k_B T$ shows that the $\omega < 0$ part of quantum spectral densities correspond to processes during which a "photon" is transferred from the impedance to the rest of the circuit while the $\omega > 0$ part corresponds to the reverse process. The quantum fluctuation–dissipation theorem constitutes a generalization of Planck's black body radiator law. The impedance plays the role of the black body radiator while the rest of the circuit plays the role of the atom. Finally the $\omega < 0$ and $\omega > 0$ processes correspond to absorption and emission processes respectively. Note that for $\omega > 0$ the $\hbar\omega\,\mathrm{Re}\,(Z[\omega])$ part of U corresponds to spontaneous emission.

3.6. Quantum fluctuations in the damped LC oscillator

How does dissipation modify the results of Eqs. (3.21) and (3.22)? We can apply the quantum fluctuation–dissipation theorem to compute the fluctuations of the damped LC oscillator of Fig. 1b. This system can be represented by the circuit diagram of Fig. 9 in which we have replaced the admittance $Y(\omega)$ by an infinite set of series LC oscillators in parallel.

Using the node variable representation we arrive at the following total Hamil-

tonian

$$\mathcal{H} = \frac{q^2}{2C} + \frac{\phi^2}{2L} + \sum_m \left[\frac{q_m^2}{2C_m} + \frac{(\phi_m - \phi)^2}{2L_m} \right]. \tag{3.31}$$

Since this Hamiltonian is quadratic we can in principle find its normal mode coordinates. However, there is a more efficient method. We can treat the circuit taken between ground and the closed dot in Fig. 9 as a dissipative element with an impedance $Z(\omega)$ given by

$$Z(\omega) = \frac{1}{\frac{1}{jL\omega} + jC\omega + Y(\omega)}. \tag{3.32}$$

Taking the spanning tree to go through the main inductance L, the node flux ϕ is identical to the flux Φ through that inductance and we get

$$\langle \Phi^2 \rangle = \frac{\hbar Z_0}{2} \int_{-\infty}^{+\infty} \frac{Z_0 \omega_0^2 \omega Y(\omega)}{\left(\omega^2 - \omega_0^2\right)^2 + Z_0^2 \omega_0^2 \omega^2 Y(\omega)^2} \coth\left(\frac{\beta\hbar\omega}{2}\right) d\omega. \tag{3.33}$$

Similarly, the conjugate charge q is identical to the charge Q on the main capacitance C and we have

$$\langle Q^2 \rangle = \frac{\hbar}{2Z_0} \int_{-\infty}^{+\infty} \frac{Z_0 \omega_0^2 \omega^3 Y(\omega)}{\left(\omega^2 - \omega_0^2\right)^2 + Z_0^2 \omega_0^2 \omega^2 Y(\omega)^2} \coth\left(\frac{\beta\hbar\omega}{2}\right) d\omega. \tag{3.34}$$

We can now apply these results to the so-called ohmic case (or resistor case) where the damping admittance is independent of frequency below a cutoff frequency ω_c which we take to be much larger than ω_0. We take $Y(\omega)$ of the form

$$Y(\omega) = \frac{1}{R + jL_c\omega} = R^{-1} \frac{1}{1 - i\frac{\omega}{\omega_c}}. \tag{3.35}$$

The integrals in Eq. (3.33) and Eq. (3.34) can be calculated in closed form [20] and one finds that in the limit $\omega_c \to \infty$, $\langle \Phi^2 \rangle$ becomes independent of ω_c. We have

$$\langle \Phi^2 \rangle = \hbar Z_0 \left\{ \theta + \frac{1}{2\pi\sqrt{\kappa^2 - 1}} \left[\Psi(1 + \lambda_+) - \Psi(1 + \lambda_-) \right] \right\} \tag{3.36}$$

where $\Psi(x)$ is the polygamma function and

$$\theta = \frac{k_B T}{\hbar\omega_0}, \tag{3.37}$$

$$\kappa = (2RC\omega_0)^{-1}, \tag{3.38}$$

$$\lambda_\pm = \frac{\kappa \pm \sqrt{\kappa^2 - 1}}{2\pi\theta}. \tag{3.39}$$

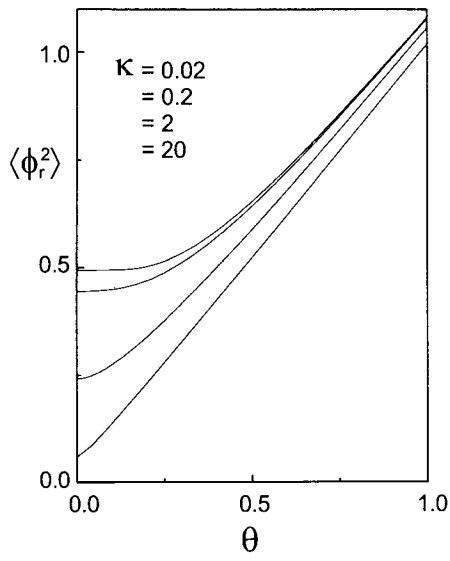

Fig. 10. Variations of the dimensionless variance $\langle\phi_r^2\rangle = \langle\Phi^2\rangle/(\hbar Z_0)$ of flux fluctuations of the LCR circuit as a function of the dimensionless temperature $\theta = k_B T/\hbar\omega_0$ for different values of the dimensionless damping coefficient $\kappa = (2RC\omega_0)^{-1}$.

In contrast with $\langle\Phi^2\rangle$, $\langle Q^2\rangle$ diverges as $\omega_c \to \infty$, a specifically quantum mechanical result. We have

$$\langle Q^2\rangle = \frac{1}{Z_0^2}\langle\Phi^2\rangle + \Delta \tag{3.40}$$

where

$$\Delta = \frac{\hbar\kappa}{\pi Z_0}\left[2\Psi(1+\lambda_c) - \frac{\lambda_+}{\sqrt{\kappa^2-1}}\Psi(1+\lambda_+) + \frac{\lambda_-}{\sqrt{\kappa^2-1}}\Psi(1+\lambda_-)\right], \tag{3.41}$$

$$\lambda_c = \frac{\hbar\omega_0}{2\pi k_B T}\left(\frac{\omega_c}{\omega_0} - 2\kappa\right). \tag{3.42}$$

These expressions are plotted in Figs. 10 and 11.

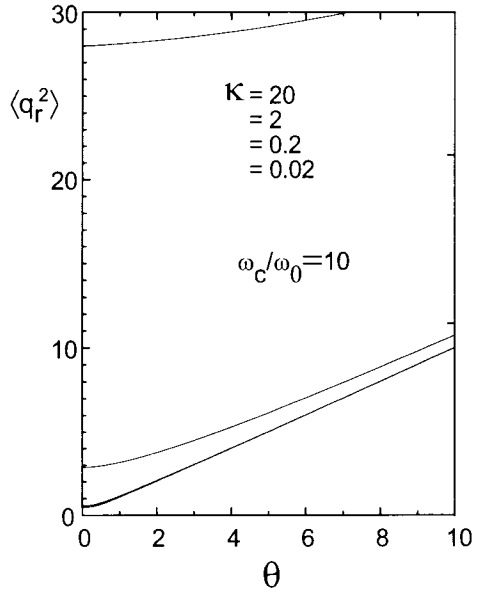

Fig. 11. Variations of the dimensionless variance $\langle q_r^2 \rangle = Z_0 \langle Q^2 \rangle / \hbar$ of charge fluctuations of the LCR circuit as a function of the dimensionless temperature $\theta = k_B T / \hbar\omega_0$ for different values of the dimensionless damping coefficient $\kappa = (2RC\omega_0)^{-1}$. For all values of κ, the cutoff frequency ω_c of the resistor has been chosen such that $\omega_c/\omega_0 = 10$. The curves for $\kappa = 0.2$ and $\kappa = 0.02$ are barely distinguishable.

3.7. *Low temperature limit*

In the limit $\theta \to 0$ we find the analytical expressions

$$\langle \Phi^2 \rangle = \frac{\hbar Z_0}{2} \frac{2 \ln \left(\kappa + \sqrt{\kappa^2 - 1} \right)}{\pi \sqrt{\kappa^2 - 1}}, \tag{3.43}$$

$$\langle Q^2 \rangle = \frac{\hbar}{2Z_0} \left[\frac{4\kappa}{\pi} \ln \left(\frac{\omega_c}{\omega_0} \right) + \left(1 - 2\kappa^2 \right) \frac{2 \ln \left(\kappa + \sqrt{\kappa^2 - 1} \right)}{\pi \sqrt{\kappa^2 - 1}} \right]. \tag{3.44}$$

It is interesting to calculate how the quantum fluctuations depend on the damping coefficient κ in the $\kappa \gg 1$ limit

$$\langle \Phi^2 \rangle = \frac{\hbar Z_0}{2} \frac{2 \ln 2\kappa}{\pi \kappa} + \mathcal{O}\left(\frac{\ln \kappa}{\kappa^3} \right), \tag{3.45}$$

$$\langle Q^2 \rangle = \frac{\hbar}{2Z_0} \frac{4\kappa}{\pi} \ln\left(\frac{\omega_c}{2\kappa\omega_0}\right) + \mathcal{O}\left(\frac{\ln\kappa}{\kappa}\right). \tag{3.46}$$

We find that the surface of the uncertainty ellipse grows logarithmically with damping

$$\sqrt{\langle \Phi^2 \rangle \langle Q^2 \rangle} \sim \frac{\hbar}{\pi} \left[2 \ln 2\kappa \ln\left(\frac{\omega_c}{2\kappa\omega_0}\right)\right]^{\frac{1}{2}} \tag{3.47}$$

an effect due to the presence of quantum degrees of freedom inside the resistor. Apart from that feature, we note that the effect of a resistor on the quantum mechanical fluctuations of the LC oscillator is essentially to rescale the size of these fluctuations. We will see in the next section that the non-linear oscillator formed by a Josephson junction can have a qualitatively distinct behavior.

4. Quantum fluctuations in superconducting tunnel junction circuits

4.1. Energy operator for a Josephson element

As we have seen in the introduction, a superconducting tunnel junction can be modeled by a pure tunnel element (Josephson element) in parallel with a capacitor. The Josephson element is such that the charge Q_J having passed through it is an integer number N times the charge $-2e$ of a Cooper pair

$$Q_J(t) = -2eN(t). \tag{4.1}$$

Quantum-mechanically, N should be treated as an operator $\widehat{N}$ whose eigenstates are macroscopic states of the circuit corresponding to well defined number of Cooper pairs having passed through the junction

$$\widehat{N} = \sum_N N |N\rangle \langle N|. \tag{4.2}$$

One can show that the tunneling of electrons through the barrier couples the $|N\rangle$ states [21]. The coupling Hamiltonian is

$$\widehat{h}_J = -\frac{E_J}{2} \sum_{N=-\infty}^{+\infty} [|N\rangle \langle N+1| + |N+1\rangle \langle N|]. \tag{4.3}$$

The Josephson energy E_J is a macroscopic parameter whose value, in the case there is the same BCS superconductor on both sides of the junction, is given by [4]

$$E_J = \frac{1}{8} \frac{h}{e^2} G_t \Delta \tag{4.4}$$

where Δ is the superconducting gap and G_t the tunnel conductance in the normal state. The tunnel conductance is proportional to the transparency of the barrier and to the surface of the junction.

4.2. The phase difference operator

Let us now introduce new basis states defined by

$$|\delta\rangle = \sum_{N=-\infty}^{+\infty} e^{iN\delta} |N\rangle . \tag{4.5}$$

The index δ should be thought of as the position of a point on the unit circle since

$$\delta \to \delta + 2\pi \tag{4.6}$$

leaves $|\delta\rangle$ unaffected.

We have conversely

$$|N\rangle = \frac{1}{2\pi} \int_0^{2\pi} d\delta \, e^{-iN\delta} |\delta\rangle \tag{4.7}$$

from which we can obtain the expression of $\hat{h}_J$ in the $|\delta\rangle$ basis

$$\hat{h}_J = -\frac{E_J}{2} \frac{1}{2\pi} \int_0^{2\pi} d\delta \left[e^{i\delta} + e^{-i\delta}\right] |\delta\rangle \langle\delta| . \tag{4.8}$$

It is natural to introduce the operator

$$e^{i\hat{\delta}} = \frac{1}{2\pi} \int_0^{2\pi} d\delta e^{i\delta} |\delta\rangle \langle\delta| \tag{4.9}$$

which is such that

$$e^{i\hat{\delta}} |N\rangle = |N-1\rangle . \tag{4.10}$$

We can thus write the coupling Hamiltonian (4.3) as

$$\hat{h}_J = -E_J \cos\hat{\delta}. \tag{4.11}$$

The operator $\hat{\delta}$ is the quantum-mechanical phase conjugate to the number operator $\hat{N}$. Note that the couple $\hat{N}$, $\hat{\delta}$ bears close resemblance to the couple formed by the number and phase operators for the mode of the electromagnetic field in quantum optics. However, it should be stressed that here the pair number operator takes its eigenvalues in the set of all integers, positive and negative, whereas the number of photon operator takes its eigenvalues in the set of non-negative integers only. We can write symbolically

$$[\hat{\delta}, \hat{N}] = i \tag{4.12}$$

being aware of the fact that due to the circle topology of the manifold $|\delta\rangle$, only periodic functions of $\widehat{\delta}$ like $e^{i\widehat{\delta}}$ have a non-ambiguous meaning.

From Eqs. (3.6) and (3.7) we have

$$\frac{d}{dt}\widehat{\delta} = \frac{1}{i\hbar}\left[\widehat{\delta}, \widehat{\mathcal{H}}\right] = -\frac{\partial}{\hbar\partial\widehat{N}}\widehat{\mathcal{H}}. \tag{4.13}$$

Since $\widehat{N}$ couples linearly to the voltage operator $\widehat{v}$ via the Cooper pair charge $-2e$, we have

$$\frac{d}{dt}\widehat{\delta} = \frac{2e}{\hbar}\widehat{v}. \tag{4.14}$$

We can thus identify $\hbar\widehat{\delta}/2e$ and the branch flux operator $\widehat{\Phi}_J$

$$\hbar\widehat{\delta}/2e = \widehat{\Phi}_J. \tag{4.15}$$

This result can also be deduced from (4.12) and the property that the Poisson bracket of a branch flux and a branch charge is unity.

Using the same type of algebra as in (4.13) and Eq. (4.11), we find that the current operator $\widehat{i} = -2ed\widehat{N}/dt$ is given by

$$\widehat{i} = I_0 \sin\widehat{\delta} \tag{4.16}$$

where

$$I_0 = \frac{2e}{\hbar}E_J. \tag{4.17}$$

Eqs. (4.15) and (4.16) form the quantum constitutive relations of the Josephson element. They could have been obtained directly by treating the Josephson element phenomenologically as a nonlinear inductance with a sinusoidal current–flux relation and by replacing the classical quantities by operators. However, the microscopic approach we have presented explains how the sine function and the flux scale $2e/\hbar$ originates from Cooper pair tunneling.

4.3. Macroscopic quantum tunneling

Let us now consider a circuit consisting of a Josephson junction with critical current I_0 and capacitance C connected to a source of current I (see inset of Fig. 12).

Such a source can be thought of as a very large inductor L_S "precharged" with a very large flux $\widetilde{\Phi}_S$ such that $\widetilde{\Phi}_S/L_S = I$. We take as degree of freedom the integral ϕ of the voltage on one plate of the capacitance C, the other plate being set to ground. In this representation, the Hamiltonian of the circuit is

$$\mathcal{H} = \frac{q^2}{2C} + \frac{\left(\widetilde{\Phi}_S - \phi\right)^2}{2L_S} - E_J \cos\frac{2e}{\hbar}\phi. \tag{4.18}$$

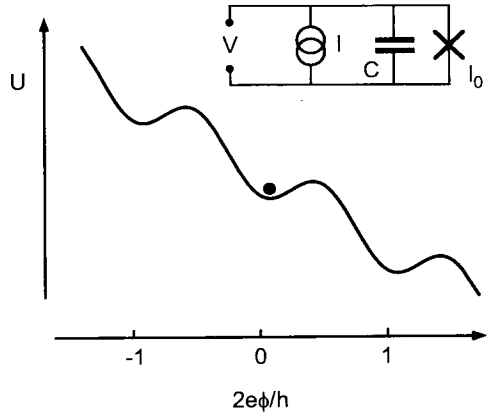

Fig. 12. A current-biased Josephson junction (inset) is equivalent to a particle in a washboard potential. The voltage V across the junction is equivalent to the velocity of the particle.

We have dropped the hat on operators. Note that the flux ϕ, in contrast to the phase difference δ, takes its values on a line and not on a circle. Likewise, its conjugate variable q, the charge on the capacitance, takes continuous values and not integer ones like N. In the limit $L_S \to \infty$, $\widetilde{\Phi}_S/L_S \to I$, the Hamiltonian (4.18) reduces to

$$\mathcal{H} = \frac{q^2}{2C} - I\phi - E_J \cos\frac{2e}{\hbar}\phi. \tag{4.19}$$

This Hamiltonian corresponds to a particle with position ϕ and mass C evolving in a washboard potential $U(\phi) = -I\phi - E_J \cos\frac{2e}{\hbar}\phi$ (see Fig. 12).

Classically, at $T = 0$ and for $I < I_0$, the particle is trapped in a potential well. Because the phase does not increase with time, the d.c. voltage V measured across the junction is then identically zero and the junction is said to be in its superconducting state. If now $I > I_0$, the washboard loses its minima and the particle rolls down the washboard. In that case $\dot{\phi}$ is non zero on average, V has a finite value and the junction is said to be in the dissipative state.

Quantum mechanically, the particle can escape even when $I < I_0$. Because the mass C is finite, ϕ can traverse the potential barrier by quantum tunneling (see Fig. 13).

This effect, named macroscopic quantum tunneling (MQT) to distinguish it from the microscopic quantum tunneling of electrons or Cooper pairs, has been observed in several experiments, along with the quantized energy levels in the washboard (see for instance the review by Devoret et al. [6]). A related effect observed recently [22] is resonant tunneling between macroscopic states of a SQUID.

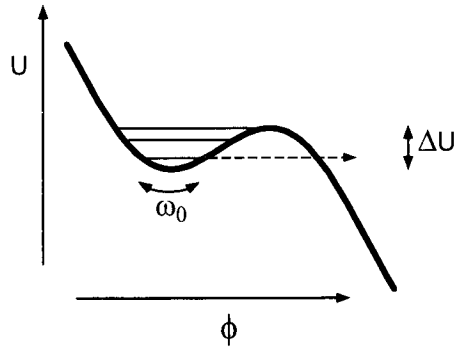

Fig. 13. Macroscopic quantum tunneling of the junction out of its superconducting state. The decay of the ground state in the well has been represented by a dashed arrow. Excited states in the well also decay by tunneling, but in practice, their main decay process is the relaxation towards lower states.

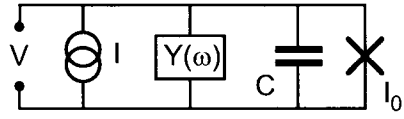

Fig. 14. Current-biased Josephson junction with its electromagnetic environment represented by an admittance $Y(\omega)$.

4.4. Influence of dissipation on macroscopic quantum tunneling

The rate of MQT in the ideal current-biased junction can be computed [1] by the WKB method and one finds an expression of the form

$$\Gamma = A \exp -B \tag{4.20}$$

where the exponent B is given for $(I_0 - I)/I_0 \ll 1$ by

$$B = 7.2 \frac{\Delta U}{\hbar \omega_0}. \tag{4.21}$$

In this last expression, ΔU is the barrier height and ω_0 the frequency of small oscillations in the well.

However, in an actual experiment, the bias current source is never perfect. There is always an admittance $Y(\omega)$ connected in parallel with the junction representing the electromagnetic influence of the leads and the filters connecting the junction placed at low temperature and the room temperature measurement apparatus (see Fig. 14).

Dissipation due to $Y(\omega)$ affects the MQT rate exponentially. For an admittance smoothly varying with frequency on the scale of ω_0 and such that $\mathrm{Re}\,[Y(\omega_0)] \ll$

$Z_0^{-1} = \sqrt{2eI_0C/\hbar}$, one can calculate using the methods discussed in sections 2 and 3 the effect of $Y(\omega)$ on B and one finds [1] that

$$B_Y = 7.2\frac{\Delta U}{\hbar\omega_0'}\left\{1 + \frac{0.87}{C\omega_0' \operatorname{Re}\left[Y(\omega_0')\right]}\right\} \tag{4.22}$$

where ω_0' is the small oscillation frequency modified by $Y(\omega)$. This expression is well-verified experimentally [6]. The effect can be understood in the following manner: as the dissipation is increased, the zero point fluctuations of the position of the particle in the well of Fig. 12 decrease in the same manner as with the harmonic oscillator and tunneling is suppressed.

4.5. Zero-voltage conductance of small Josephson junctions

Junctions used in MQT experiments are large in the sense that the Josephson energy E_J giving the scale of the barriers in the washboard potential is large compared with the scale $E_C = (2e)^2/2C$ of the energy of zero-point fluctuations in the well of the washboard. As the size of the junction is reduced, both C and I_0 tend to become smaller and the ratio E_J/E_C diminishes. For E_J/E_C of order unity, the particle tends to diffuse quantum-mechanically along the washboard potential. In this regime, the sinusoidal non-linearity of the potential becomes a crucial feature. Although the relation between the voltage across the junction and the bias current is presently not fully understood in this regime, it is still possible to calculate the zero-bias conductance of the system for $Y(\omega) = R^{-1}$ [23].

One calculates the conductance from the Fourier transform of the correlation function of the current operator

$$G \sim \lim_{V\to 0}\frac{1}{V}\int_0^\infty dt\,\langle[i(t), i(0)]\rangle \exp(-2ieVt/\hbar)\,. \tag{4.23}$$

This involves as an intermediate step the computation of the important quantity

$$P(E) = \int_0^{+\infty} dt\left\langle e^{i2e\phi(t)/\hbar}e^{-i2e\phi(o)/\hbar}\right\rangle \exp(-iEt/\hbar) \tag{4.24}$$

which is the probability that during tunneling a Cooper pair excites the electromagnetic environment with an energy E. In this last expression ϕ is the flux across the admittance as in the damped LC circuit of section 3. Since

$$\left\langle e^{i2e\phi(t)/\hbar}e^{-i2e\phi(o)/\hbar}\right\rangle = e^{-(2e/\hbar)^2\langle[\phi(t)-\phi(0)]\phi(0)\rangle} \tag{4.25}$$

one deduces from Eq. (3.25) that the ratio R/R_Q where $R_Q = (2e)^2/h$ will play a critical role in the $t \to \infty$ limit of the integral of (4.24). At $T = 0$ one finds that for $R > R_Q$ the diffusion of ϕ becomes unbounded and $G = 0$ (insulating state) whereas for $R < R_Q$ the diffusion of ϕ is suppressed, ϕ is

localized around one well and $G = \infty$ (superconducting state). There is now good experimental evidence for such effects [24]. Dissipation, which tends to suppress the fluctuations of ϕ and make it more classical, actually favors superconductivity!

4.6. Circuits with islands

We consider now circuits in which junctions are connected to other junctions or to capacitors. One junction electrode at least will form an isolated superconducting "island", a node whose charge q_n can vary only by electron tunneling. When the even–odd free energy of this island is greater than the electrostatic energy $e^2/2C_\Sigma$ corresponding to one excess electron [25], then the charge q_n will adopt the values $-2en$ where n is an integer. Here C_Σ denotes the total capacitance of the island. Note that the node flux ϕ_n conjugate to q_n here takes its values on a circle and coincides, apart from the factor $\hbar/2e$ with the phase of the superconducting electrons in the island.

Furthermore, if $(2e)^2/2C_\Sigma$ is greater than the Josephson energy of the junctions leading to this island, the number n of Cooper pairs will be a good quantum number while the conjugate flux ϕ_n will be completely uncertain quantum-mechanically. This is the regime of Josephson effects with one Cooper pair [26,27]. From the point of view of node fluxes one is in a quantum regime analogous in quantum optics to situations where the number of photons in a cavity is a good quantum number [5]. The interplay between the electrostatic energy which tends to fix the number of pairs on islands and the Josephson energy which tends to induce quantum fluctuations of the island pair number lead to new collective quantum phenomena in circuits containing several junctions and junction arrays [10,28].

Acknowledgements

This course has greatly benefited from discussions with V. Bouchiat, D. Esteve, H. Grabert, G.-L. Ingold, P. Joyez, P. Lafarge, H. Pothier, S. Reynaud and C. Urbina. The author is also indebted to P. Chauve and S. Bos for their contribution to the section on the Hamiltonian description of an arbitrary non-linear circuit. Financial support has been, in part, provided by the Bureau National de la Métrologie.

References

[1] A.J. Leggett in: *Chance and Matter*, J. Souletie, J. Vannimenus and R. Stora eds. (Noth-Holland, Amsterdam, 1987) Course 6.

[2] *Quantum Tunneling in Condensed Media*, Y. Kagan and A.J. Leggett eds. (Elsevier, Amsterdam, 1992).

[3] At microwave frequencies, impedances tend to be of the order of the impedance of the vacuum $Z_{vac} = (\mu_0/\epsilon_0)^{1/2} \simeq 377\ \Omega$.
[4] B.D. Josephson in: *Superconductivity*, R.D. Parks, ed. (Marcel Dekker, New York, 1969) Chap. 9.
[5] J.M. Raimond and S. Haroche, Course 8, this volume.
[6] M.H. Devoret, D. Esteve, C. Urbina, J. Martinis, A. Cleland and J. Clarke, in: *Quantum Tunneling in Condensed Media*, Y. Kagan and A.J. Leggett, eds. (Elsevier, Amsterdam, 1992) [ref. 2].
[7] K.K. Likharev, *Dynamics of Josephson Junctions and Circuits* (Gordon and Breach, New York, 1986).
[8] *Single Charge Tunneling*, H. Grabert and M.H. Devoret, eds. (Plenum, New York, 1992).
[9] *Mesoscopic Superconductivity*, F.W.J. Hekking, G. Schön and A.V. Averin, eds. (Elsevier, Amsterdam, 1994).
[10] *Macroscopic Quantum Phenomena and Coherence in Superconducting Networks*, C. Giovanella and M. Tinkham, eds. (World Scientific, Singapore, 1995).
[11] Proceedings of the NATO ASI meeting on *Mesoscopic Electron Transport*, Curacao June 25–July 5 (1996).
[12] B. Yurke and J.S. Denker, Phys. Rev. A **29** (1984) 1419.
[13] The exact condition for the existence of conjugate momenta for each node flux is that there be no nodes connected only to inductances and that the sub-network of capacitances be connex.
[14] H. Goldstein, *Mechanics* (Addison-Wesley, New York, 1980).
[15] R. P. Feynman, *Lectures on Physics* (Addison-Wesley, Reading, 1964) Vol. 2, Chap. 23.
[16] A.O. Caldeira and A.J. Leggett, Ann. Phys. (N.Y.) **149** (1983) 374.
[17] U. Weiss, *Quantum Dissipative Systems* (World Scientific, Singapore, 1993).
[18] P.A.M. Dirac, *The Principles of Quantum Mechanics* (Oxford University Press, Oxford, 1967).
[19] R. Kubo, Rep. Prog. Phys. **29** (1966) 255.
[20] H. Grabert, U. Weiss and P. Talkner, Z. Phys. B **55** (1984) 87.
[21] P.G. de Gennes, *Superconductivity of metals and alloys* (Benjamin, New York, 1966).
[22] R. Rouse, S. Han and J.E. Lukens, Phys. Rev. Lett. **75** (1995) 1614.
[23] G.-L. Ingold and Y. Nazarov in: *Single Charge Tunneling*, H. Grabert and M.H. Devoret, eds. (Plenum, New York, 1992) [ref. 8].
[24] L. Kuzmin et al. in: Proceedings of the NATO ASI meeting on *Mesoscopic Electron Transport*, Curacao June 25–July 5 (1996) [ref. 11].
[25] M.T. Tuominen et al., Phys. Rev. Lett. **69** (1992) 1997; Lafarge et al., Nature **365** (1993) 422.
[26] W.J. Elion et al., Nature **371** (1994) 594.
[27] P. Joyez et al., Phys. Rev. Lett. **72** (1994) 2458; V. Bouchiat, Ph.D. thesis (Paris VI, 1997).
[28] H.S.J. Van der Zant et al., Phys. Rev. Lett. **69** (1992) 2971.